Model-Based Estimation of Intracranial Pressure and Cerebrovascular Autoregulation

FM Kashif, T Heldt, GC Verghese

Massachusetts Institute of Technology, Cambridge, MA, USA

Abstract

Monitoring cerebrovascular state, including intracranial pressure (ICP) and the ability to regulate cerebral blood flow, is important for patient care in stroke, traumatic brain injury and other such conditions. However, current methodologies for direct measurement of ICP are highly invasive, and expose patients to the risk of infection. In addition, vascular properties such as resistance and compliance cannot be directly assessed. In this work, we employ a mathematical model-based approach to track variations in ICP and cerebrovascular properties from signals that can be acquired entirely non-invasively. The performance on simulation data indicates that the estimates track the desired quantities closely, thus suggesting that tests using clinical data are warranted.

1. Introduction

Brain tissue cannot withstand ischemic conditions: neurological symptoms appear within seconds of reduced oxygen delivery, and if ischemic conditions prevail for a few minutes, there is a high risk of irreversible damage to brain function [1]. To maintain the desired local blood supply, the cerebral vasculature has the innate ability to respond to pressure and flow changes by altering the diameters of arterioles and by altering the compliance of arteries. In humans, this cerebral autoregulation acts to maintain a steady cerebral blood flow (CBF) in the face of arterial blood pressure (ABP) variations in the range of 50-150 mmHg [1].

Perfusion to the brain also directly depends on intracranial pressure (ICP), which alters cerebral perfusion pressure through the Starling resistor mechanism acting at the level of cerebral veins [2]. The plateau-wave phenomenon, where ICP rapidly rises and stays elevated for a period of at least a few minutes, remains the subject of research due to its association with poor patient outcome [3].

Several pathological conditions can affect the cerebral vasculature and its autoregulatory ability. In ischemic stroke or intracranial hemorrhage, for example, blood supply to the brain tissue is disrupted. Vascular diseases may impair intracranial compliance or may block the absorption of fluid from the cranial into the vascular space, leading to an increased intracranial fluid volume. The cerebral vasculature might fail to maintain the desired blood supply either due to an impaired cerebral autoregulation, for example in premature neonates [4], or because intracranial conditions are beyond its autoregulation capacity.

To monitor patient state and provide appropriate therapeutic intervention, continuous monitoring of ICP and the state of cerebral autoregulation is critical. However, current methods for direct measurement of ICP are highly invasive, require considerable expertise, and pose the risk of infection [5]. ICP measurement is therefore not routinely done. The estimation of resistance and compliance in a model for CBF regulation is described in [6], though not aimed at ICP estimation or real-time monitoring.

In this work, we develop a mathematical model-based approach to perform beat-by-beat estimation of ICP, cerebrovascular resistance and arterial compliance, to aid in diagnosis and therapy. We adapt a well-established model [7] to capture the pulsatile behavior of the associated variables. The model is then simplified, and estimation algorithms are developed. These estimation algorithms utilize ABP and CBF measurements, both of which can be obtained entirely non-invasively. The performance on simulated data is presented.

2. Methods

Initial model

A physiological model that is well-established and widely used in the research community is the one proposed by Ursino and Lodi [7], a simplified version of their detailed model [8]. The model is represented by an electrical circuit analog. We make the following two modifications to this Ursino-Lodi model to obtain the representation in Fig. 1.

Modification I: The model of [7] operates on mean quantities, i.e., cycle-averaged pressures and flows, and all the model relationships, including control mechanisms for

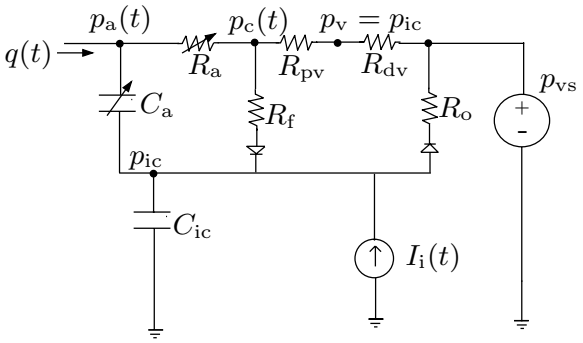

Figure 1. The adapted cerebrovascular model.

varying resistance and compliance, are expressed in terms of these averages. We instead allow the model to operate on *pulsatile* pressure and flow waveforms. However we still use cycle-averaged quantities to drive the control mechanisms (as these mechanisms tend to respond to averaged rather than instantaneous quantities); averages are computed using running-windows of duration equal to one or more beats.

Modification II: The model [7] labels the flow through the arterial resistance $R_{\rm a}$ of the cerebral vasculature as the CBF. We instead take the flow $q(t)$ at the *input* of the model to be the CBF, since measurements of CBF are typically obtained at the level of the middle cerebral arteries, upstream of the arterial bed.

The remaining components of the model in Fig. 1 have the following interpretation. Intracranial space is modeled by a compliance, $C_{\rm ic}$. The arterial portion of the cerebral vasculature is modeled by a compartment with compliance $C_{\rm a}$, and resistance $R_{\rm a}$. Cerebrospinal fluid (CSF) formation at the level of the capillaries is represented by a high resistance pathway $R_{\rm f}$, taking flow into the intracranial space. Similarly, outflow of CSF is represented by another high resistance pathway $R_{\rm o}$, that drains into the venous sinuses at a pressure $p_{\rm vs}$. The venous segment is modeled by two resistances corresponding to the proximal and distal segments around the venous collapse that results from ICP being higher than $p_{\rm vs}$. The Starling resistor model for this phenomenon leads us to equate the pressure $p_{\rm v}$ at the point of collapse with ICP, labeled as $p_{\rm ic}$ in the figure. The current source $I_{\rm i}(t)$ represents external injection of CSF into the intracranial space. A first-order feedback, exactly as in [7] but not shown in Fig. 1, acts to maintain a steady flow through $R_{\rm a}$.

Model simplification

The model of Fig. 1 is a second-order system with nonlinear components and specified by eight parameters. In clinical environments, we expect to have only two (highly correlated) measurement signals, ABP and CBF, which makes it infeasible to obtain reliable estimates for all the model parameters. Moreover, we do not really need to know all the parameters; we are concerned with only the ones that are relevant to determining ICP and autoregulation. Hence, we need to simplify the model. Below we develop one such simplification based on time-scale separation of important cardiovascular dynamics. This is only one of a handful of possible reduced models originating from the modified Ursino-Lodi model. Other reduced models for the cerebrovascular system are possible and can be treated similarly.

Our model simplification is based on the following observations about the model in Fig. 1.

Observation I: The resistances associated with CSF formation and reabsorption pathways, $R_{\rm f}$ and $R_{\rm o}$ respectively, are at least two orders of magnitude higher than the arterial-arteriolar resistance. Therefore, the flow through these pathways is negligible compared to the arterial flow. Since we are interested in analyzing the model at the time-scale of the beat interval, we can safely remove these high resistance paths.

Observation II: Intra-beat ICP variations are much smaller compared to the intra-beat ABP variation. Moreover, significant changes in the mean level of ICP occur at a longer time-scale than a beat period. Therefore, for intra-beat analysis, ICP can be assumed to be approximately constant.

These two observations reduce the original second-order model into a first-order model, shown in Fig. 2. We have combined $R_{\rm a}$ and $R_{\rm pv}$ into a single resistance, renaming it as $R_{\rm av}$. The simplified system can be described by the following differential equation:

$$q(t) = C_{\rm a}\frac{dp_{\rm a}(t)}{dt} + \frac{1}{R_{\rm av}}\left[p_{\rm a}(t) - p_{\rm ic}(t)\right]. \qquad (1)$$

Thus the estimation task is reduced to only determining two parameters, $C_{\rm a}$ and $R_{\rm av}$ as well as the unknown node pressure $p_{\rm ic}$. We describe the estimation algorithm in the next section.

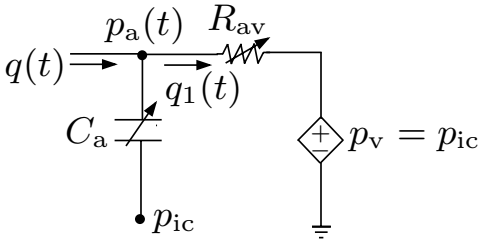

Figure 2. The simplified model.

Estimation algorithm

Given access to the ABP waveform $p_{\rm a}(t)$ and CBF waveform $q(t)$, we describe a two-stage estimation scheme

for the model parameters.

Step I: Sharp transitions in $p_{\rm a}(t)$ induce a large flow into the arterial compliance, and there is negligible flow through the resistance branch during such transitions if they occur over short enough periods. The typical ABP waveform does indeed contain a sharp rise — within about one-tenth of a beat period — from diastolic pressure to systolic pressure in every beat. Hence, during that short transition period, the input flow can be primarily attributed to the compliance branch:

$$q(t) \approx C_{\rm a} \frac{dp_{\rm a}(t)}{dt}. \tag{2}$$

Let $t_{\rm b}$ and $t_{\rm s}$ indicate the beginning and end of the sharp transition, respectively, in a particular beat of ABP waveform $p_{\rm a}(t)$. We can estimate $C_{\rm a}$ by integrating (2) over the transition period, as below:

$$\widehat{C}_{\rm a} = \frac{\int_{t_b}^{t_s} q(t)dt}{p_{\rm a}(t_s) - p_{\rm a}(t_b)}. \tag{3}$$

Step II: Using the result of the estimation in Step I and again ignoring ICP variations over the duration of a single beat, we can calculate the flow through the arterial resistance as

$$\widehat{q}_1(t) = q(t) - \widehat{C}_{\rm a} \frac{dp_{\rm a}(t)}{dt}. \tag{4}$$

Note that direct computation of the derivative involved above may accentuate noise in the ABP waveforms. In our simulation experiments, we used an experimental ABP waveform as the input; simple finite-differencing provided an adequate approximation of the derivative. In more noisy cases, a more careful approximation scheme will need to be used.

Assuming that the resistance stays constant over a beat interval, ICP can be computed using $\widehat{q}_1(t)$ as

$$p_{\rm ic}(t) = p_{\rm a}(t) - R_{\rm av}\widehat{q}_1(t). \tag{5}$$

Still assuming ICP stays approximately constant within a beat, we can estimate $R_{\rm av}$ from (5) using $\widehat{q}_1(t)$ and $p_a(t)$ evaluated for at least two time instants t. For example, by picking t_1 and t_2 within a beat, (5) yields

$$\widehat{R}_{\rm av} = \frac{p_{\rm a}(t_2) - p_{\rm a}(t_1)}{\widehat{q}_1(t_2) - \widehat{q}_1(t_1)}. \tag{6}$$

To reduce sensitivity to the noise in $\widehat{q}_1(t)$, it is advantageous to pick t_1 and t_2 to lie near the maximum and minimum of the ABP waveform so that $\frac{dp_{\rm a}(t)}{dt} \approx 0$ in (4). With this choice the estimate of $R_{\rm av}$ is minimally dependent on the estimate of $C_{\rm a}$.

Returning to (5) now gives the desired ICP estimate:

$$\widehat{p}_{\rm ic}(t) = p_{\rm a}(t) - \widehat{R}_{\rm av}\widehat{q}_1(t). \tag{7}$$

To provide smoother estimates of $\widehat{C}_{\rm a}$ and $\widehat{R}_{\rm av}$, we can average over several consecutive beats.

3. Results

The performance of our estimation scheme is analyzed using simulated waveforms. To generate data for our analysis purposes, we supply an experimental ABP waveform as input to the modified Ursino-Lodi model in Fig. 1, with the control loop operational. Model parameters are set to the nominal values specified in [7]. To represent some of the phenomena of clinical interest, such as intracranial hypertension and plateau waves [3, 5], we choose appropriate perturbations on $I_{\rm i}$ in Fig. 1. We simulate the model and record the waveform samples of pressure and flow throughout the model, including ICP and CBF.

In one of the simulation runs, $I_{\rm i}$ was set to 1.5 ml/sec at $t = 10$ sec for a duration of 10 seconds, and then to 3 ml/sec at $t = 40$ sec for a duration of 5 seconds, and the model was simulated for an experimental ABP waveform provided as the input. Cycle-averaged ABP, CBF and q_1 (i.e., flow through $R_{\rm a}$) are shown in Fig. 3. We also record cerebrovascular resistance and arterial compliance, which represent the regulatory mechanism. The dashed lines in Fig. 4 show the beat-by-beat values of compliance, resistance and ICP obtained from the simulation for this particular run. Resistance is seen to have a rapid change at about $t = 160$ sec. This variation corresponds to a sudden drop in the input mean ABP around that time. ICP increases rapidly to about 40 mmHg at $t = 10$ sec, and to 45 mmHg at $t = 40$ sec due to the input perturbations.

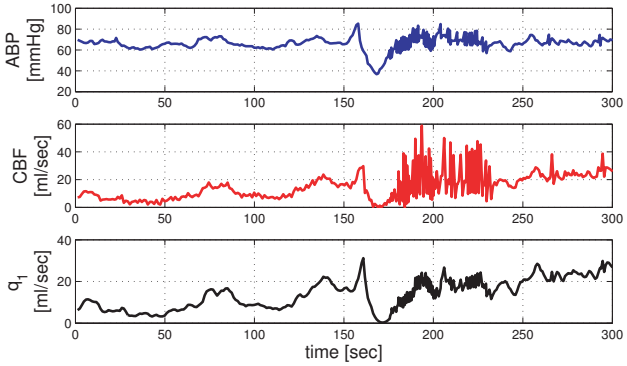

Figure 3. Simulation data: cycle-averaged ABP, CBF, and q_1 (flow through $R_{\rm a}$) are shown (top to bottom).

Taking the ABP and CBF waveforms from the simulation as the available data, beat-by-beat estimates of $C_{\rm a}$, $R_{\rm av}$ and ICP are obtained in accordance with the estimation algorithm outlined above. The results for the simulation run in Fig. 4 are shown in solid lines. The estimates for compliance and resistance generally have less than 5% and 10% error, respectively. The ICP estimates also track the simulated ICP closely.

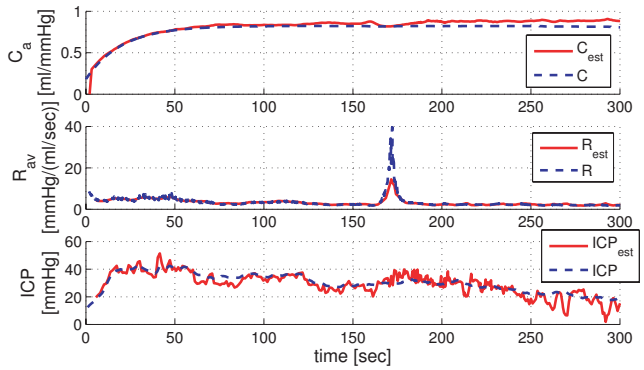

Figure 4. Estimation performance: beat-by-beat values of C_a, R_{av} and ICP are shown, where the blue (dashed) lines correspond to the simulated values, and the estimates are shown in red (solid) lines.

4. Discussion and conclusions

The dispersion in the estimation results of the above section is caused by the signal quality, the algorithm choices (such as the time indices selected in the algorithm), and the assumptions made to simplify the model. Signal quality depends on the sampling rate and the noise in the waveforms. The sampling rate of the waveforms determines the timing jitter in the discrete-time indices for beat-onset detection and for marking t_{s}, t_1 and t_2; a low sampling rate adds more noise to these marker locations. The results presented above were obtained for a sampling rate of 125 Hz. Noise in the measurements degrades the estimation performance, e.g., it makes the approximation of the derivative in (4) poorer. Another algorithm choice is the window length for averaging the resistance and compliance estimates. A larger window serves to average out the noise better but can degrade tracking of the transients. A window length of 5 beats was used in the results presented above.

In clinical environments, the measurements of ABP and CBF pose some potential problems for our proposed approach.

1. ABP and CBF measurements are not available at the same location. CBF is usually measured at the middle cerebral artery via a Doppler-based method, while ABP is generally measured at the radial artery or finger. Consequently, the pressure and flow waveforms are shifted with respect to each other, which therefore calls for a synchronization step before estimation. Also, the peripheral ABP morphology is different from what would be seen at the middle cerebral artery. Since our estimation scheme primarily utilizes the pulse-pressure information from the ABP waveform rather than actual morphology, the main effect is expected to be a scaling of the estimates, but this remains to be investigated farther.

2. CBF is calculated from blood velocity measurement by assuming a nominal value or an estimate of the diameter of the middle cerebral artery. This is another potential source of error in estimates, needing further investigation.

Clinical testing of the estimation approach described here seems warranted. Such testing may point to necessary refinements of the model. For example, intracranial conditions may be such that only a subset of the cerebral veins are in collapsed state. In this case, the Starling resistor assumption in the model would need to be modified. Finally, variations in resistance, compliance and ICP will need to be tied more closely to the efficacy of autoregulation.

Acknowledgements

The authors would like to thank MIT and the Center for Integration of Medicine and Innovative Technology (CIMIT) in Boston for a Biomedical Engineering Fellowship awarded to FMK. This work was supported in part by the National Institute of Biomedical Imaging and Bioengineering of the National Institutes of Health through grant R01 EB 001659. We would also like to thank Dr. Vera Novak at Boston's Beth Israel Deaconess Medical Center for helpful discussions at the beginning of this work.

Address for correspondence:
George C. Verghese, `verghese@mit.edu`
Room 10-140K, MIT, Cambridge, MA 02139, USA.

References

[1] Kandel ER, Schwartz JH, Jessell TM. Principles of Neural Science. New York: McGraw Hill, 2000.

[2] Chopp M, Portnoy HD. Starling resistor as a model of the cerebrovascular bed. In Intracranial Pressure, 5th ed. Berlin: Springer-Verlag, 1983; 174–179.

[3] Hayashi M, Handa Y, Kobayashi H, Kawano H, Ishii H, Hirose S. Plateau-wave phenomenon (I) and (II). Brain 1991; 114:2681–2699.

[4] De Bor M, Walther FJ. Cerebral blood flow velocity regulation in preterm infants. Biol Neonate 1991;59:329–335.

[5] Lundberg N. Continuous recording and control of ventricular fluid pressure in neurosurgical practice. Acta Psych Neurol Scand 1960;36(Supplement 149):1–193.

[6] Olufsen MS, Nadim A, Lipsitz LA. Dynamics of cerebral blood flow regulation explained using a lumped parameter model. Am J Physiol 2002;282:R611–R622.

[7] Ursino M, Lodi CA. A simple mathematical model of the interaction between intracranial pressure and cerebral hemodynamics. J Appl Physiol 1997;82:1256–1269.

[8] Ursino M, Lodi CA. A mathematical study of human intracranial hydrodynamics parts 1 and 2. Ann Biomed Eng 1988;16(4):379–416.